Seismic Imaging of the Dead Sea rift and Jordan Valley for Seismic Hazard and Resource Evaluation

Uri Ten-Brink and Zvi Ben Avraham and, The Dr. Moses Strauss Department of Marine Geosciences, the Leon H. Charney School of Marine Sciences, University of Haifa.
Eldad Levi, the Geophysical Institute of Israel, Lod.

July 2019

Abstract

The main objective of the research was to obtain an image of the Dead Sea fault sub-surface geometry and a map of the sub-surface seismic velocities along the axis of the basin to a depth of 15-20 km at a resolution of ≥1 km.

Two perpendicular wide angle seismic refraction / reflection cross-sections were acquired in order to image the Dead Sea fault structure in the northern part of Israel; A west-east line, from the Mediterranean coast line near Acre in the west to the Syrian border in the Golan Heights in the East with total length of 72 km; A south-north line, from Kibbutz Kfar Rupin in the south to Almagor village in the north crossing the Sea of Galilee with total length of 50 km. The seismic energy sources were 12 underground explosive shots, 300–400 kilograms each located every ~10 km, while the 550 seismic receivers were located every ~200m along the lines.

The results are 13 shot gathers showing medium to poor quality data. The dataset was not interpreted completely yet. First results of refraction waves give a penetration depth of about 8 km probably imaging the crystalline basement.

Project field work

The research proposal included a 90-km-long south-north line along the axis of the Dead Sea and the lower Jordan Valley. The proposed line could not be carried out with the current budget, because of the unexpected costs involved in marine work in the Dead sea. With approval from the Lounsbery Foundation, the research area was moved to the northern part of Israel. The goals of the research, namely, understanding the crustal and sedimentary structure in the vicinity of the Dead Sea transform plate boundary in northern Israel crossing the Sea of Galilee, with implications to seismic hazard and resource exploration, remained, however, the same.

The data acquisition was carried along two perpendicular lines (figure 1):

1. A west-east line, from the Mediterranean coastline near Acre in the west to the Syrian border in the Golan Heights in the East with total length of 72 km.
2. A south-north line, from Kibbutz Kfar Rupin in the south to Almagor village in the north crossing the Sea of Galilee with total length of 50 km.

There is a lot of interest understanding the northern part of the Dead Sea fault. The Bible and historical and archeological records document numerous earthquakes along the Dead Sea fault. The largest to strike Israel in recent history was the magnitude 7.1 Safed earthquake, which occurred on January 1, 1837, killing more than 5,000 people and causing massive damage to cities and villages. The latest reminder of seismicity in the region was a series of small earthquakes early last July, located in the Sea of Galilee, the largest of which had a magnitude of 4.5

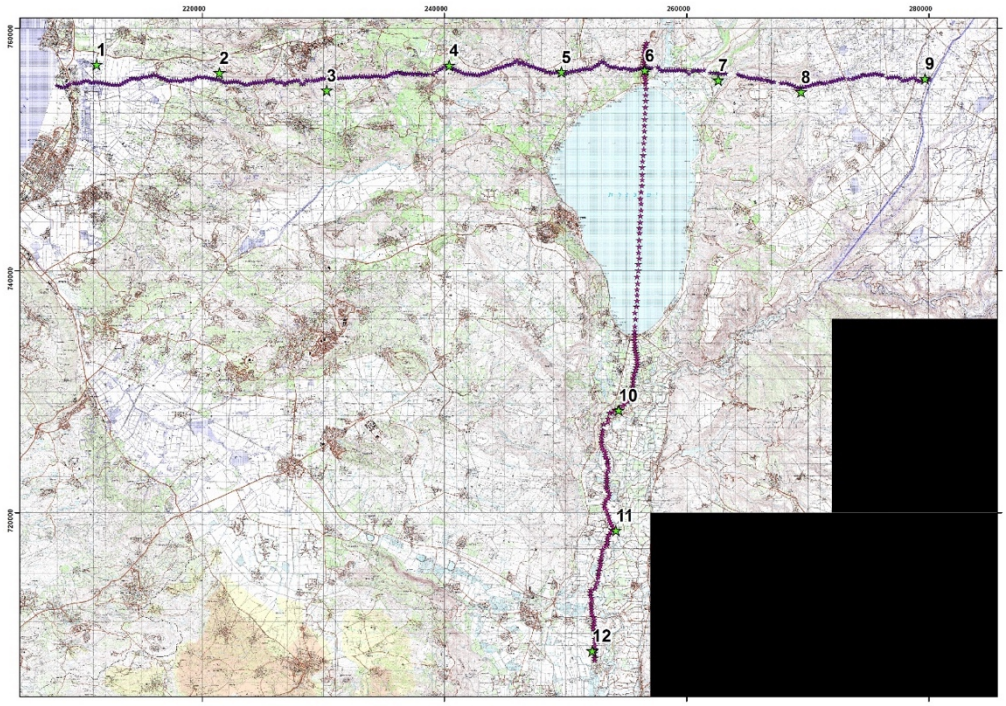

Figure 1 – Location map of the seismic lines, Texans (pink) and shots (green, numbered).

Pre-survey preparation

Coordination

The following entities were contacted for coordination, following the planning of the acquisition parameters and timetable:

- Israel Defense Forces – for entering and deploying equipment in military training areas and the next to the Jordanian border.
- Israel Nature Reserves Authority – for permission to deploy equipment in Nahal Hilazon.Natural Reserve.
- Israel Antiquities Authority – Drilling in Antiquities-declared areas must be supervised by the authority.
- Towns and villages where the boreholes were drilled.
- Ministry of Labor - for permits for explosives use.
- Nine Regional Councils where the seismic lines were located.
- Beeper LTD – to disconnect the pre-earthquake alert in schools in the adjacent of some explosions to avoid their triggering.
- Sea of Galilee fishermen – information about the equipment deployment in the lake.
- Customs authorities – to import the seismic equipment necessary for the experiment.

Drilling

Twelve boreholes were drilled to host underground explosions. The boreholes were located every 6-10 km along the lines, 9 holes along the east-west line, and 3 holes on the south-north line (figure 1). Borehole #6 was located at the intersection of the two perpendicular lines.

The boreholes were drilled during 6 days as follow: March 25th - boreholes 2 and 3; March 26th - boreholes 4 and 5; March 29th - boreholes 10,11 and 12; April 1st - borehole 1; April 3rd - boreholes 6,7 and 8; April 4th - borehole 9.

The boreholes were drilled with foundation-construction drilling rigs to depths of 16-18 meters and a diameter of 45 cm. Boreholes located in limestone, dolomite and basalt rocks (boreholes 2-9) were drilled with micro piles drilling rig, whereas boreholes drilled into clay soils (1,10-12) were drilled using bucket auger rig (figure 2).

Boreholes 1 and 12 were located in places with shallow water table, and were therefore drilled with bentonite and cased with wide diameter plastic pipe (40 cm). The pipes were inserted into the boreholes to prevent collapse.

The water table was encountered during drilling in 3 additional boreholes:

- Borehole 10 - water was encountered at ~10 m depth. The borehole collapsed at deeper depth so two additional boreholes of 10m depth were drilled a few meters apart;
- Borehole 8 - water was encountered at ~10 m depth, but it did not collapse and the borehole was drilled to 16 m;
- Borehole 9 - water was encountered at ~3 m depth. It was drilled to 14m, but a plastic tube was not inserted. This borehole subsequently collapsed to a depth of 9 m.

Figure 2 – Bucket auger drilling rig mounted on a truck, bentonite tanker and the plastic pipe, at borehole #12.

Survey

All receiver locations on land were pre-surveyed and marked by GII surveyor teams with RTK GPS – Garmin R10 during 8 days between 20th – 29th of March. The teams also marked all the tracking routes in the area. All pre-surveyed data were uploaded to the GPS units of the deployment teams. The deployment teams made an effort to locate the Texan units in a vicinity to the pre-surveyed locations. In addition, the teams took a GPS reading with hand-held GPS at every deployment location.

After the survey, all deployment locations were compared with the pre-surveyed points and a final receiver location file was created.

Data acquisition

Hardware

The data was recorded with 550 Texan dataloggers RT125A (figure 3) (https://www.passcal.nmt.edu/content/instrumentation/dataloggers/1-channel-texan-dataloggers)

which were loaned for the survey by the IRIS-Passcal Instrument Center and shipped to Israel. IRIS-Passcal is a non-profit organization funded by the U.S. National Science Foundation to provide logistical support for seismological research. The Texans dataloggers are compact single channel dataloggers with a self-contained power supply, and can record continuously for approximately 120 hours.

510 of the Texan units were deployed with 4.5 Hz Geosapce GS-11D geophones (Figure 3) every approximately 200 m on land whereas the other 40 units were deployed with 10 Hz hydrophones Geospace MP-25 (figure 4) in the Sea of Galilee.

In order to use the land datalogger at the marine environment, "homemade" sealed buoyant plastic tube were built to keep the datalogger dry. The hydrophones were hanged on 50 cm length side screw to prevent contact between the hydrophone and the rope which anchored the unit to the lake floor (figure 4). The tubes were made of Geberit 110-mm-thick plastic pipe about 30 cm long. The tube parts were connected by unique plastic welding, making the tube totally waterproof. A plastic bag with sand had to be inserted into the tube to keep it vertical while floating.

Figure 3- Texan RT125A (left) and Texan connected to Geospace GS-11D 4.5 Hz geophone**.**

Table 1 - Geospace GS-11D geophone specifications.

PHSICAL SPECIFICATIONS	
Orientation	Vertical and Horizontal avaliable
Moving Mass	23.6 g
Maximum Coil Excursion p-p	> 2.5 mm
Diameter	3.18 cm
Height	3.35 cm
Weight	118 g
Operating & Storage Temperature Range	$-45^0$to + 85^0 C
ELECTRICAL SPECIFICATIONS	**at 25^0 C**
Frequency	4.5 Hz
Spurious Frequency	N.S.
Distortion at Vertical	N.S.
Coil Resistance	380 Ohm
Open-Circuit Sensitivity	32.0 V/m/s
Sensitivity at 70% damping	26.18 V/m/s
Open-Circuit Damping	34%
Tilt angle when coil hits end stop	Vertical geophone = 16^0 | Horizontal geophone +- 1.25^0

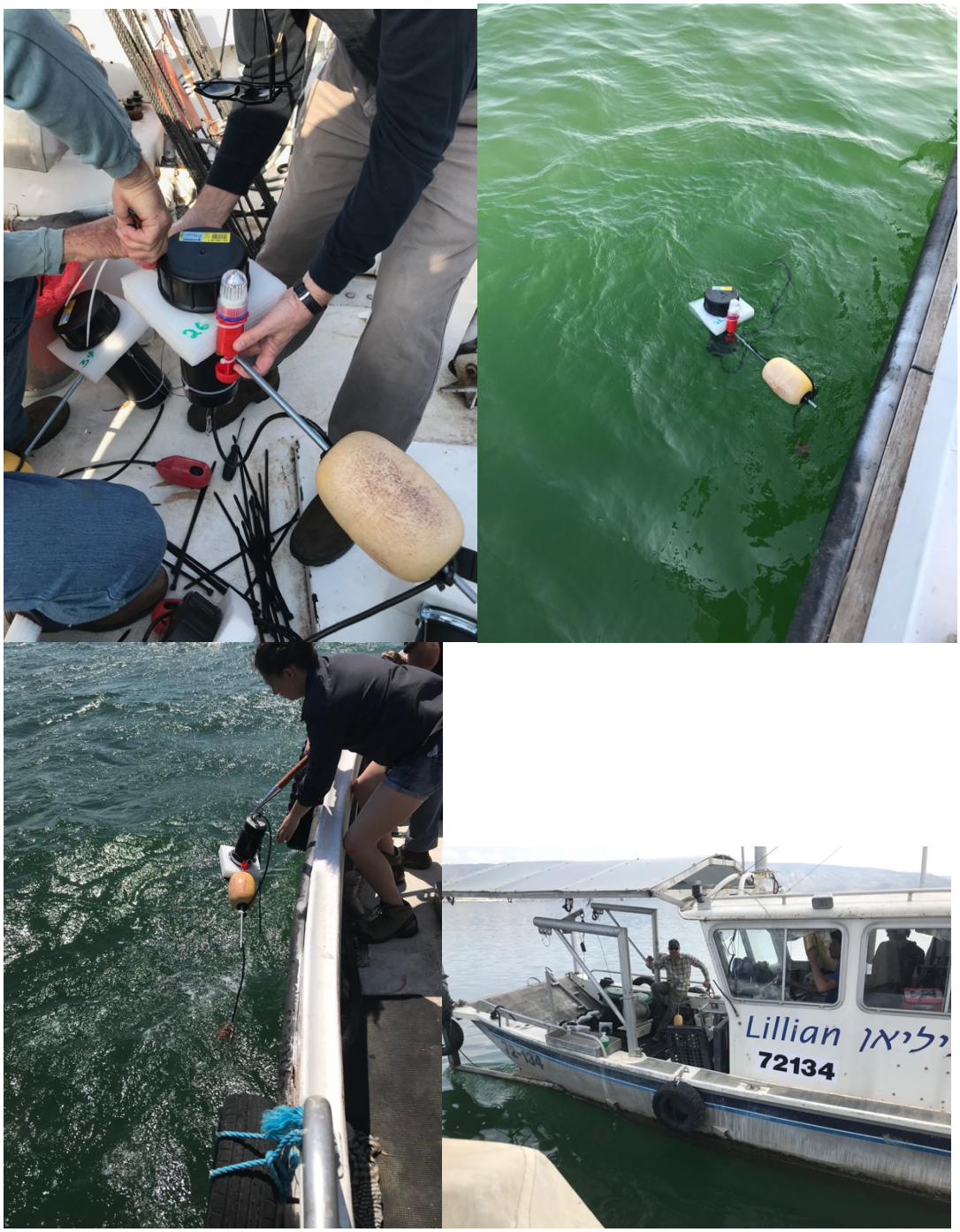

Figure 4 – A floatation tube with the hydrophone and a flasher being prepared for deployment (top left), deployed at the lake (top right) and being picked up (bottom left). Bottom right - The R/V Lillian, one of the deployment boats, during work on the lake.

Table 2- Geospace mp-25 hydrophone specifications.

DIMENSIONS	**with Outer Case**
Length	13.97 cm
Diameter	6.10 cm
Weight	349 g
PHYSICAL SPECIFICATIONS	
Operating Temperature	0-35 C^0
Operatinal Depth	0.3-76.2 m
ELECTRICAL SPECIFICATIONS	
Natural Frequency	10 Hz
Voltage Sensitivity	11.2 Volts/bar
Impedance	250 Ohm
DC Resistance	160 Ohm

All the marine units were equipped with an Arduino GPS datalogger, and in addition 15 units were equipped GPS trackers (GTA-04) which sent their locations via the cellular network every 30 seconds.

Deployment / Pickup

All the Texan units were moved to Kibbutz Moran on April 5th. There they were programmed to record continuously from April 9th 16:00 UTC to April 11th 16:00 UTC, at a sampling rate of 4 ms intervals.

Figure 5 – Eldad Levi and Lloyd Carothers (IRIS-Passcal) programming the Texans.

The land receivers were deployed during two days (April 8th and 9th) by 5 GII teams, each team included 2-3 people and a pickup truck. The receivers were picked up by the same teams on the 11th of April and on the morning of the 12th of April. The marine receivers were deployed using two ILOR boats, the R/V Hermona and Lillian on the 9th of April and were picked up by the R/V Lillian on the 11th of April.

Although each land unit was deployed in a small trench and covered with soil, a few units were found by local people. In most cases the people who found the unit informed GII after reading the labels with contact information, that were attached to each receiver, but in one case the police was involved and the unit was retrieved from the police station in Rosh Pina. During Pick up about twenty units were found outside the trench probably dug out mostly by animals.

Two units in the Sea of Galilee, located at Stations 2008 and 2012, were lost. It is suspected that the wire that connected the unit and the rope was too weak and broke during the afternoon wind and waves. One of the units was found floating by chance on April 17th by the ILOR team.

Deployments sheets of the teams were scanned and attached to the report as .pdf files.

Figure 6 – Deployment (left) and recovery (right) of a Texan receiver unit**.**

Sound sources

Detonation of underground explosions took place during the daylight hours of the 10th of April. Explosives for all the shots arrived from Explosives Manufacturing Industries LTD. The explosives arrived to the area in one truck and were divided to three teams, each led by an authorized explosions expert (figure 6). Each team shot four holes during the day.

The dry holes were shot with 400 kg of Anfo type explosives whereas the water-saturated holes were shot with 300 kg of emulsion explosives. Source #9 where the hole collapsed to a depth.

Figure 7 – Explosives load: Anfo type explosive (left), and emulsion type (right).

of 9 m, was shot with only 120 kg of emulsion. Explosives at source #11 were divided between the two adjacent drill holes. After loading the explosives each hole was filled up with small gravel limestones and the cuttings left by the drilling operation. The explosions at the two shallow drilled holes (#11 and #9) created a blowout and left craters. The ground in those locations was subsequently filled and restored by bulldozers. Borehole 5 encountered a cavity at the bottom of the hole, owing likely to karst, affecting thee coupling of the explosion energy to the rock.

The shooting system (figure 7) connected a high precision GPS clock with a capitative discharge blasting machine. The energy of the blasting machine is 4 Joules at 400 V. The GPS clock generates a pulse every UTC minute and when the blasting machine part of the system is charged and connected to the clock the blasting machine produces a 400 V pulse. The system was designed and built at University of Texas El Paso (UTEP). There are no commercial companies manufacturing this sort of equipment.

Table 3- Sound source metadata**.**

Source no.	Team	Name	Location	rock type	Water saturated	X	Y	amount (kg)	Explosive type	Depth (m)	shot time (UTC)
1	1	West Galilee1	Ein Hamifratz	beach rock	yes	32.908056	35.119444	300	emulsion	17	12:25:00
2	1	West Galilee2	Sha'ab	limestone	no	32.900446	35.225213	400	anfo	15	7:51:00
3	1	Central Galilee1	Tzvia	limestone	no	32.887546	35.319244	400	anfo	15	9:14:00
4	1	Central Galilee2	Hazon	limestone	no	32.906786	35.42724	400	anfo	15	6:15:00
5	2	East Galilee1	Kahal	limestone	no	32.900887	35.527162	400	anfo	15	8:18:00
6	3	East Galilee2	Almagor	basalt	no	32.902753	35.599851	400	anfo	15	7:58:00
7	2	Golan 1	Yonatan packing	basalt	no	32.895943	35.666192	400	anfo	15	9:53:00
8	2	West Golan	Nes 6 hole	basalt	yes	32.885649	35.737952	300	emulsion	15	11:40:00
9	2	East Golan	Garania	basalt	yes	32.89133	35.834597	120	emulsion	8	13:13:00
10	3	Jordan Valley North	Ashdot Yaakov	clay	no	32.649812	35.575925	400	anfo	18	10:04:00
11	3	Jordan Valley Central	Yardena	clay	yes	32.555521	35.56606	300	emulsion	10	11:50:00
12	3	Jordan Valley South	K. Rupin	clay	yes	32.470981	35.551148	300	emulsion	17	13:31:00

Figure 8 – GPS time controlled shooting box.

Passive seismic recording

Data was collected over 48 hours, from the 9th of April 16:00 UTC to the 11th of April 16:00 UTC. During that time 62 events recorded by GII's seismological network, 12 of them are our shots.

An example of an earthquake offshore Lebanon is shown belo.

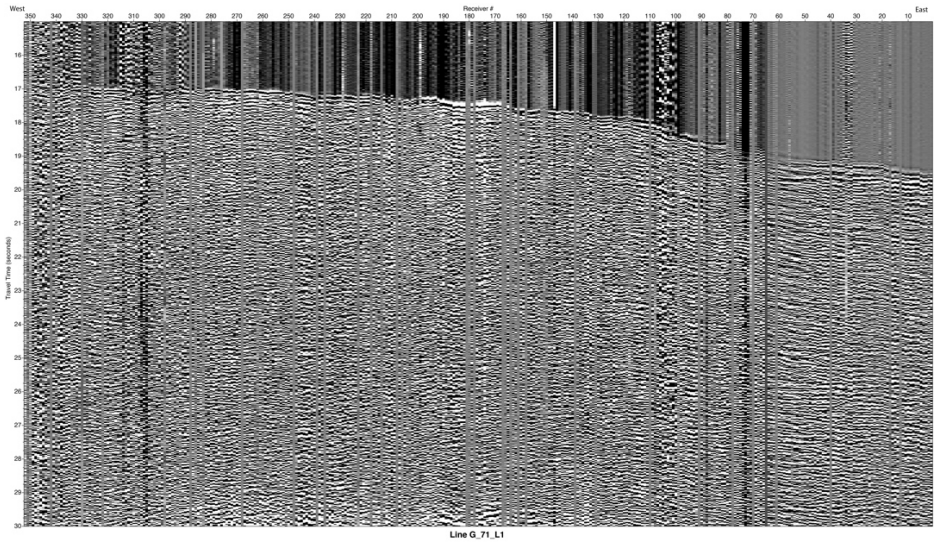

References

Al-Zoubi, A. S., T. Heinrichs, I. Qabbani, and U. S. ten-Brink (2007), The northern end of the Dead Sea basin; geometry from reflection seismic evidence, Tectonophys., 434, 55-69.

Arbenz, J. K. (1984), Oil potential of the Dead Sea area, *Rep. 84/11,* Seismica Oil Exploration, Tel Aviv.

Ben-Avraham, Z., and G. Schubert (2006), Deep "drop down" basin in the southern Dead Sea, Earth Planet. Sci. Lett., 251(3-4), 254-263, doi: 10.1016/j.epsl.2006.09.008.

Braeuer, B., G. Asch, R. Hofstetter, C. Haberland, D. Jaser, R. El-Kelani, and M. Weber (2012), Microseismicity distribution in the southern Dead Sea basin and its implications on the structure of the basin, Geophysical Journal International, 188(3), 873-878.

Gardosh, M., E. Kashai, S. Salhov, H. Shulman, and E. Tannenbaum (1997), Hydrocarbon exploration in the southern Dead Sea basin, in The Dead Sea: The lake and its setting, edited by T. M. Niemi, Z. Ben-Avraham and J. R. Gat, pp. 57-72, Oxford University Press, Oxford.

Garfunkel, Z. (1981), Internal structure of the Dead Sea leaky transform (rift) in relation to plate kinematics, Tectonophys, 80, 81-108.

Garfunkel, Z., and Z. Ben-Avraham (1996), The structure of the Dead Sea basin, Tectonophys, 266, 155-176.

Ginzburg, A., and Z. Ben-Avraham (1997), A seismic refraction study of the north basin of the Dead Sea, Israel, Geophysical Research Letters, 24(16), 2063-2066, doi: 10.1029/97gl01884.

Ginzburg, A., M. Reshef, Z. Ben-Avraham, and U. Schattner (2007), The style of transverse faulting in the Dead Sea basin from seismic reflection data: The Amazyahu fault, Isr. J. Earth Sci., 55, 129-139.

Kashai, E. L., and P. F. Croker (1987), Structural geometry and evolution of the Dead Sea-Jordan rift system as deduced from new subsurface data, Tectonophys., 141, 33-60.

Lazar, M., Z. Ben-Avraham, and U. Schattner (2006), Formation of sequential basins along a strike-slip fault; geophysical observations from the Dead Sea basin, Tectonophys., 421(1-2), 53-69, doi: 10.1016/j.tecto.2006.04.007.

Levi, E., U. ten Brink, and Z. Ben-Avraham, (2019) Wide angle seismic refraction survey across the Dead Sea fault and along Jordan Valley, northern Israel, Israel Geological Society Annual Meeting, Kfar Blum, March 2019.

Mechie, J., K. Abu-Ayyash, Z. Ben-Avraham, R. El-Kelani, I. Qabbani, and M. Weber (2009), Crustal structure of the southern Dead Sea basin derived from Project DESIRE wide-angle seismic data, Geophysical Journal International, 178(1), 457-478.

Neev, D., and J. K. Hall (1979), Geophysical investigations in the Dead Sea, Sedimentary Geology, 23, 209-238.

Petrunin, A. G., E. Meneses Rioseco, S. V. Sobolev, and M. Weber (2012), Thermomechanical model reconciles contradictory geophysical observations at the Dead Sea Basin, Geochem., Geophys., Geosystems, 13(4).

Shamir, G. (2006), The Active Structure of the Dead Sea Depression, Geol. Soc. Am. Spec. Pap., 401, 15-32.

Shamir, G., Y. Eyal, and I. Bruner (2005), Localized versus distributed shear in transform plate boundary zones; the case of the Dead Sea Transform in the Jericho Valley, Geochem., Geophys., Geosystems, 6(5), doi: 10.1029/2004gc000751.

Steckler, M. and ten Brink, U., (1986). Lithospheric strength variations as a control on new plate boundaries: examples from the northern Red Sea region, Earth and Planetary Science Letters, 79, 120

Sykes, L.R., Intraplate seismicity, reactivation of preexisting zones of weakness, alkaline magmatism and other tectonosim postdating continental fragmentation; Rev. Geophys. Space Phys. 16, 621-688.

ten Brink, U. S., and Z. Ben-Avraham (1989), The anatomy of a pull-apart basin: Seismic reflection observations of the Dead Sea basin, Tectonics, 8(2), 333-350.

ten Brink, U. S., Z. Ben-Avraham, R. E. Bell, M. Hassouneh, D. F. Coleman, G. Andeasen, G. Tibor, and B. Coakley (1993), Structure of the Dead Sea pull-apart basin from gravity analysis, J. Geophys. Res., 98(B12), 21887-21894.

ten Brink, U., M. Rybakov, A. Al-Zoubi, M. Hassouneh, A. Batayneh, U. Frieslander, V. Goldschmidt, M. Daoud, Y. Rotstein, and J.K. Hall, (1999). The anatomy of the Dead Sea plate boundary: Does it reflect continuous changes in plate motion? Geology, v. 27, pp. 887-980.

ten Brink, U. S., A. S. Al-Zoubi, C. H. Flores, Y. Rotstein, I. Qabbani, S. H. Harder, and G. R. Keller (2006), Seismic imaging of deep low-velocity zone beneath the Dead Sea basin and transform fault; implications for strain localization and crustal rigidity, Geophysical Research Letters, 33(24), L24314, doi: 10.1029/2006gl027890.

ten Brink, U. S., and C. H. Flores (2012), Geometry and subsidence history of the Dead Sea basin: A case for fluid□induced mid□crustal shear zone?, J. Geophys. Res., 117(B1).